High Power Laser Science and Engineering, (2020), Vol. 8, e33, 6 pages.
doi:10.1017/hpl.2020.33

HIGH POWER LASER SCIENCE AND ENGINEERING

LETTER

Greater than 2 kW all-passive fiber Raman amplifier with good beam quality

Yizhu Chen, Tianfu Yao, Hu Xiao, Jinyong Leng, and Pu Zhou

College of Advanced Interdisciplinary Studies, National University of Defense Technology, Changsha 410073, China

(Received 1 July 2020; revised 4 August 2020; accepted 12 August 2020)

Abstract

We report a 2 kW all-fiberized Raman fiber amplifier with efficient brightness enhancement based on the graded-index fiber. The maximum power output reaches up to 2.034 kW centered at 1130 nm, with a conversion efficiency of 79.35% with respect to the injected pump power. To the best of our knowledge, this is the highest conversion efficiency obtained for any Raman laser system using graded-index fiber. An optimized fiber combiner adopting graded-index fiber as the pigtail fiber was fabricated, enabling the preservation of the seeding brightness in the core-pumped Raman fiber amplifier, and further enhancing the ultimate brightness of the output laser after amplification. At the maximum power output, the beam quality parameter M^2 is 2.8, corresponding to a signal-to-pump brightness enhancement factor of 11.2. As far as we know, we obtain the highest brightness enhancement among Raman fiber lasers of over 100 W, and the best beam quality for graded-index Raman fiber lasers of over 150 W.

Keywords: nonlinear optics; optical fiber lasers; power amplifiers; Raman scattering

1. Introduction

The fiber laser has undergone rapid development, with outstanding properties in terms of power output, brightness and optical efficiency[1, 2]. Remarkable progress has further promoted diverse applications in the fields of manufacturing industry, medical science, remote sensing and communications. At the time of writing, the most common implementation is based on active fibers such as Yb-doped fiber, boosting the record for power scaling to greater than 10 kW[3–5]. Another way to obtain high-power laser output is the Raman fiber laser (RFL), which employs the stimulated Raman scattering (SRS) effect in a piece of passive fiber without any rare-earth dopants[6–8]. Compared with Yb-doped fiber lasers (YDFLs), the most attractive feature of the RFL is wavelength flexibility. It can emit across almost the whole spectrum of transparency of a silica window, in particular beyond the emission band of rare-earth-doped fiber lasers[9–19].

The power scaling of continuous-wave RFLs has recently reached 2 kW, with a best beam quality factor M^2 of ~8.9[20]. It is, however, challenging to achieve high beam quality at this power level, especially when the enlarged fiber core is employed to suppress second-order Stokes light. In fact, the output beam quality of high-power RFLs can also be good enough to meet practical requirements, based on brightness enhancement (BE) employing either cladding-pumping double-clad or multi-clad fibers[21–23], or core-pumping graded-index (GRIN) fibers[12, 18–20]. In the former scheme, the coupled pump light in the cladding is converted into the Stokes laser transmitted through the core of fiber to obtain BE. The power record for cladding-pumped RFL is 1.2 kW, and the corresponding M^2 is 2.75 with a BE of ~7[23]. The manufacture of these unique Raman fibers is usually complicated and costly, however, the cladding-to-core area ratio required is small (< 8) to suppress high-order Stokes light, imposing a limitation upon BE capacity based on the currently available pump brightness[24].

As an economical substitute, core-pumping GRIN fiber has an advantage over beam clean-up effects for enhancing the output brightness without complex design of the fiber structure[25, 26]. With the rapid advancement of high-power laser diodes (LDs), it was feasible to directly apply LD pumping in the GRIN RFLs for BE. Yao *et al*. proposed an LD-pumped RFL in 2015, obtaining a 20 W laser from GRIN fiber with an M^2 that was improved from 22 to 5,

Correspondence to: P. Zhou, College of Advanced Interdisciplinary Studies, National University of Defense Technology, Changsha 410073, China. Email: zhoupu203@163.com

and a BE of 5.2[27]. In 2016, Glick *et al*. reported an LD-pumped RFL based on GRIN fiber[28], and the maximum power output reached 154 W with an M^2 of 8 and a BE of 3 through optimizing the fiber length[29]. Zlobina *et al*. also studied RFL based on GRIN fiber, and the beam quality was quite good with an M^2 of ~1.2 and a BE of ~40, and the demonstrated power was 10 W[18].

The fabrication of fiber Bragg gratings (FBGs) directly on the GRIN fiber enables the selection on the fundamental mode, further boosting the BE based on all-fiberized RFLs[30]. The maximum power of LD-pumped GRIN RFL reached 62 W, and the M^2 was 3 with a BE of 25[31]. Using the customized FBGs, the all-fiber GRIN RFL pumped by fiber lasers obtained 135 W power with an M^2 of 2.5 and a BE of 5.6[32]. In general, the employment of FBGs written on GRIN fiber enabled all-fiber RFL with not only improved efficiency but also higher BE, with an M^2 improved to 2–3. The process for manufacturing FBGs with multimode (MM) GRIN fibers is relatively complex, however, it is challenging to further scale the power output with good beam quality through the resonant cavity.

To obtain power boosting without the critical requirements of MM GRIN FBGs, one can use the master oscillator power amplifier (MOPA) system, where a relatively low-power oscillator with stable properties is applied as the seed source. The MOPA system has shown significant potential for high-power and high-brightness laser generation based on rare-earth dopants. Furthermore, the abilities of Raman amplification based on MOPA have been proved in recent years[20, 33–35]. In 2018, our group employed a high-power combiner and proposed an all-fiber Raman fiber amplifier (RFA) based on GRIN fiber, whose power output was 528.8 W with an M^2 of ~4.2 and a BE of 3.8[33]. Not long after, the power output was improved to 1002.3 W through optimizing the fiber length, with an M^2 of 5.06 and a BE of 2.6[34]. Most recently, the power output of the RFA was improved to 2 kW, while the poor input seed brightness and serious thermal effects resulted in apparent beam spot distortion, preventing the BE process, and the best beam quality M^2 was only 8.9[20]. The power scaling capacity of the RFA has been proven, but more research and discussion are still required to simultaneously achieve high BE and good beam quality at this power level.

To explore efficient BE in high-power RFAs employing GRIN passive fiber, the optimization of seed injection was adopted. We demonstrated an RFA with an optimized input seed beam quality M^2 of 3.37, which is ~4.7 times higher than that in previous work[20]. The RFA employs a MOPA, and the maximum power is 2.034 kW with a conversion efficiency of 79.35%. The beam quality parameter M^2 at maximum power output is ~2.8, with a BE of ~11.2, which is the best beam quality for GRIN RFLs of over 150 W. Thanks to the improved input and output brightness with fewer transverse modes, the beam fluctuation caused by thermal effects has also been greatly suppressed. Meanwhile, this system gives the highest BE parameter for high-power Raman lasers with over 100 W power.

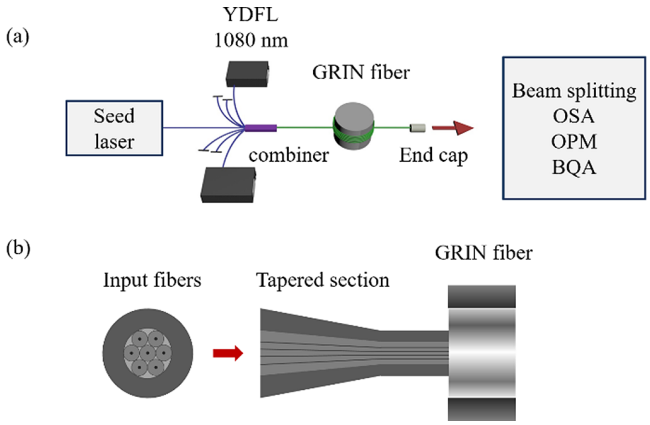

Figure 1. Raman fiber amplifier experimental setup. (a) Implementation of the amplifier; (b) cross-section through the input fiber bundles and the fusion point of the pump and signal combiner (PSC). BQA, beam quality analyzer; OPM, optical power meter; OSA, optical spectrum analyzer.

2. Experiment

As described in Figure 1(a), the RFA comprises a master oscillator as the seed laser and combined fiber lasers as the pump for the amplifier. The oscillator is an RFL at 1130 nm pumped by a YDFL at 1080 nm. The power of the input seed is 153 W, which includes 135 W signal laser at 1130 nm and 18 W unconverted pump laser at 1080 nm. The pump lasers of the amplifier stage are YDFLs at 1080 nm. The output fibers of the seed and pump lasers all feature core and inner-cladding diameters of 20 μm and 400 μm, respectively.

In order to ensure high-power transmission efficiency as well as conservation of the injected seed beam quality at the same time, a $(6+1)\times 1$ pump and signal combiner (PSC) was optimally fabricated, employing the same GRIN fiber in the amplifier stage as the output fiber. The core and cladding diameters of all seven input fibers are 20 μm and 130 μm, respectively. The output fiber of the PSC has core and cladding diameters of 62.5 μm and 125 μm, respectively, and the numerical aperture (NA) of the core is 0.275. The cross-section of the input bundles and the fusion point are shown schematically in Figure 1(b). The conventional PSC, which has been widely applied in cladding-pumped fiber lasers and amplifiers, utilizes the pump and signal laser beams injected separately into the cladding and core of double-clad fiber[36–38]. The PSC in our work, however, is designed to combine the pump and signal lasers together into the core of the GRIN fiber. Thus, to maximize preservation of the seed beam quality, the central fiber of the tapered bundles, which has been accurately fixed at the center of the bundles, is employed for seed injection. The parameters

https://doi.org/10.1017/hpl.2020.33 Published online by Cambridge University Press

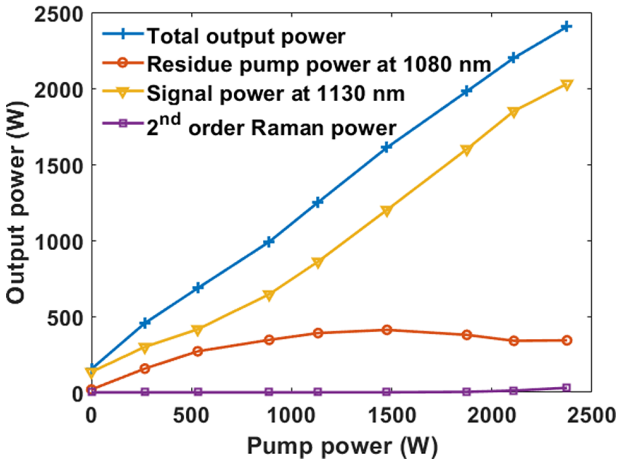

Figure 2. The power output characteristics of the RFA based on GRIN fiber, including total power output, residual pump power at 1080 nm, signal power at 1130 nm and second-order Raman power.

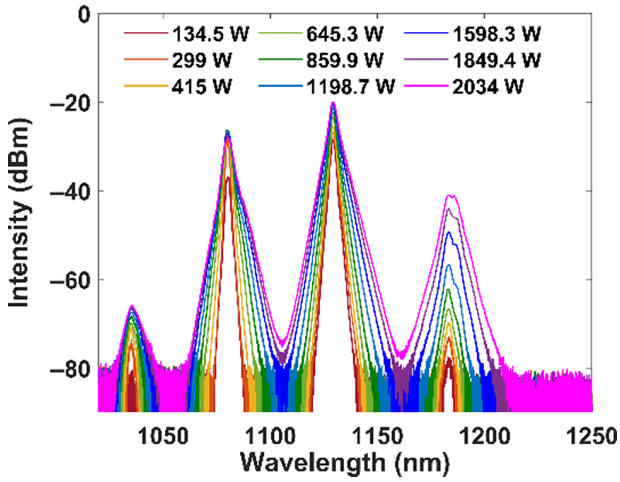

Figure 3. The spectrum of a Raman amplifier for various signal laser power outputs.

for tapering and splicing during the PSC fabrication process were simulated and optimized to achieve precise alignment and to minimize the mismatching of mode fields of lower-order modes. The powers of the seed and pump lasers after the PSC are measured individually by an optical power meter (OPM) with high power endurance. The insertion losses of the PSC for the seed (153 W) and pump (3 kW) are separately measured to be less than 5%.

Another piece of GRIN fiber was then spliced with the pigtail GRIN fiber of the PSC, these two fibers having identical parameters. The total length of the GRIN fiber in the RFA is ~20 m, which has been optimized to suppress the higher-order Raman light. At the far end of the GRIN fiber, an end cap is employed to ensure safe lasing and the elimination of backward reflection. For removal of the thermal load, the fibers are coiled around a metal barrel whose temperature is maintained at ~20°C.

3. Results

The power output of the amplifier as a function of the launched pump power is shown in Figure 2, and the total power output rises almost linearly with increasing pump laser power. The maximum total power output of the amplifier reaches 2405 W at 2375 W launched pump power. Accordingly, the maximum power of the signal laser at 1130 nm is 2034 W. The conversion efficiency (with respect to the launched pump power) and the slope efficiency are 79.36% and 83.05%, respectively. The residual pump power increases initially, and then gradually decreases to 341.5 W at the maximum power output. The second-order Raman laser shows a notable increase when the signal laser power is ~1980 W, and grows to 29.6 W at maximum power.

The output spectra of the amplifier are illustrated in Figure 3. In the seed laser, there is only pump laser at 1080 nm and signal laser at 1130 nm. Through power amplification, the spectral intensity of the signal laser keeps improving. The second-order Stokes light centered at 1183 nm appears in the seed laser. It increases along with the amplification process, but the power is too low to be calculated when the signal power is lower than 1980 W. At the maximum power output, the peak intensity of higher order Stokes light is ultimately ~20.95 dB lower than that of the signal. The spectral component centered at 1036 nm rises nearly simultaneously with the higher order Raman light and increases at a slow rate. This phenomenon could be attributed to the four-wave-mixing effect, in which two photons at different wavelengths are consumed, generating photons at two other wavelengths[6]. The power of the 1036 nm laser component remains very low for various signal power levels. The full width at half maximum (FWHM) bandwidth of the seed laser is 1.88 nm, which grows to 3.16 nm at the maximum power output. The broadening of various spectral portions is related to the nonlinear effects in the GRIN fiber[39]. Meanwhile, the amplified first- and second-order Stokes lights show different spectral shapes. The first-order Stokes light centered at 1130 nm is seeded by the launched seed laser, and pumped by the 1080 nm laser. Thus, the first-order Stokes light is amplified based on wavelength selection centered at 1130 nm, resulting in a regular spectral shape similar to the seeding spectrum. By contrast, the second-order Raman light increases based on spontaneous Raman scattering. The Raman noise serves as the seed for the second-order Stokes light, and the signal laser at 1130 nm is utilized as the pump. In this case, the Raman gain of the second-order Stokes laser is based on the typical Raman gain spectrum in silica fiber, resulting in a similar spectrum shape for the second-order Stokes laser[6].

The beam qualities of the signal laser and pump laser with respect to the output signal power are measured by a

https://doi.org/10.1017/hpl.2020.33 Published online by Cambridge University Press

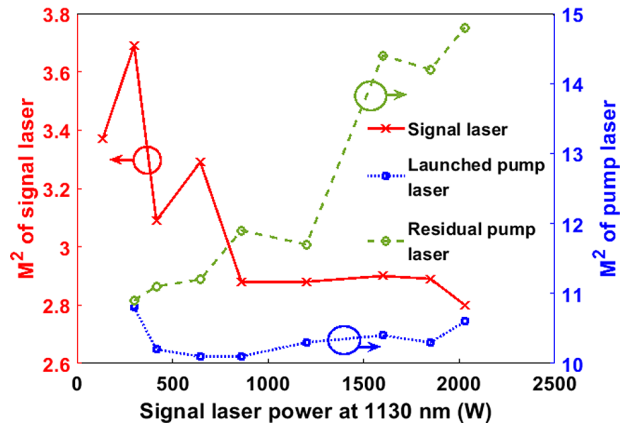

Figure 4. The beam quality parameter M^2 of the output laser with varying output signal laser power, including the amplified signal laser, the launched pump laser, and the residual pump laser.

beam quality analyzer (BQA), and are depicted in Figure 4. After the PSC, the M^2 of the launched pump laser at varying power levels remains between 10.1 and 10.8. The M^2 of the seed laser after the PSC is ~3.37, which is much better than the seeding beam quality of ~15.84 in the previous demonstration[20]. This improvement can be attributed to the optimization of seed injection accomplished by the optimized PSC. Note that there is a fluctuation in the M^2 curve of signal laser at a power lower than 1 kW. According to the power endurance of the BQA, different sets of lenses are applied to attenuate the incremental signal laser to an appropriate power level for measurement. At a power lower than 1 kW, multiple adjustments are applied to the free-space optical path according to the increasing power of the signal laser, inevitably resulting in measurement error. With power scaling of the amplifier, the M^2 of the signal laser shows an overall tendency toward improvement, thanks to the BE process, and finally reaches ~2.8 at the maximum power. As far as we know, this is the best beam quality for a 2 kW-level Raman laser in any kind of configuration with BE. In Figure 4, the M^2 of the residual pump light degrades gradually from 11 to ~14.8 with respect to the incremental signal laser power. This implies that the Raman conversion is accomplished by the portion of pump laser with brighter beam quality.

4. Discussion

Laser brightness (B) is defined as the laser power per unit area and per unit solid angle, and it can be expressed as[2]

$$B = \frac{P}{\left(M^2 \cdot \lambda\right)^2}, \tag{1}$$

where P is the laser power and λ is the wavelength. In the amplifier, the value of BE represents the ratio of the signal output brightness to the launched pump brightness, as shown

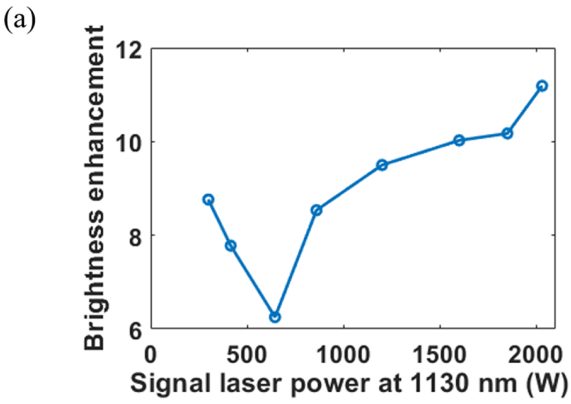

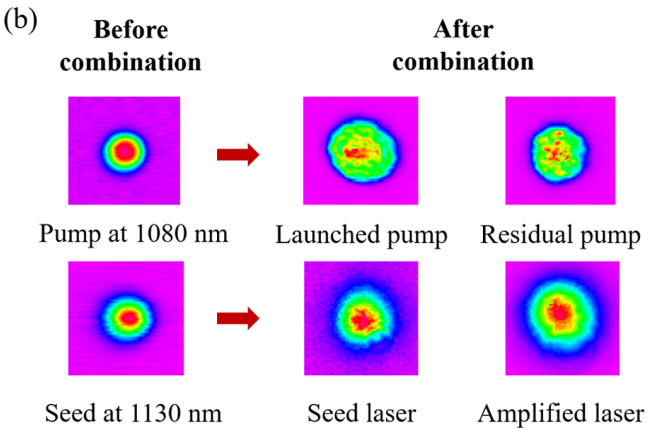

Figure 5. (a) The BE value and (b) the beam shape at the focal spot in the BQA, including the seed and pump lasers before the PSC; and the seed laser, the signal laser at maximum power, the launched pump laser at maximum power and the residual pump laser at maximum power after the PSC.

in Figure 5(a). When the signal laser power increases from 299 W to 645 W, the BE value decreases from 8.8 to 6.3. This is due to insufficient Raman conversion at the beginning of amplification. With a constantly increasing low-brightness pump power, the power of the high-brightness signal laser increases at a slower rate, resulting in a decrease of BE, according to Equation (1). This can also be proved by the relatively low slope efficiency in Figure 2. When more pump laser is launched, the Stokes shifting is more efficient, and the high-brightness signal laser power grows rapidly. Correspondingly, the BE value increases to ~11.2 at the maximum power output. This BE value is higher than in any previous high-power BE-enabled Raman lasers (over 100 W power output). Figure 5(b) shows the beam shapes at the focal spot in the BQA. Before the PSC, the beam spots of the pump and seed lasers have regular Gaussian-like profiles. After the PSC, the beam shape of the seed laser remains, whereas those of the launched and residual pump laser degrade. At maximum power, the beam spot of the amplified signal laser is also Gaussian-like and symmetric, indicating that the optimization of the launched seed laser is effective to guide the amplification of the high-brightness laser.

https://doi.org/10.1017/hpl.2020.33 Published online by Cambridge University Press

Table 1. Recent high-power Raman lasers based on GRIN fiber and output performance[40].

Number	Configuration	Pump source	Power	M^2	BE	Efficiency	Reference
1	Resonator	LD	50 W	2.6	25	27%	[30]
2	Resonator	LD	154 W	8	3	65%	[29]
3	Resonator	Fiber laser	135 W	2.5	5.6	68%	[32]
4	Resonator	LD	62 W	3	25	30%	[31]
5	Amplifier	Fiber laser	2087 kW	8.9		59.3%	[20]
6	Amplifier	Fiber laser	2034 kW	2.8	11.2	79.3%	This work

In the experiment we achieved a significant improvement of output beam quality in a 2 kW RFA compared with the previous result[20]. This can be attributed to the optimal design of the power combination and seed injection. In the amplifier, a homemade 7×1 combiner is employed, whose output fibers is a piece of step-index fiber (SIF). The core and cladding diameters of the input and output fibers are 20 μm and 400 μm, and 50 μm and 360 μm, respectively, with a core NA of the output fiber of ~0.22. The pigtailed step-index fiber is incompatible with the GRIN fiber serving as a Raman fiber, however. The mode field mismatching goes against achieving good beam quality of the seed laser, and a good beam quality of the seed laser is hard to maintain. Thus, the SIF pigtailed power combiner without additional design of seeding beam quality optimization cannot ensure superior BE in the amplifier.

Table 1 shows the experimental results for several of the latest high-power RFLs based on GRIN fiber, as mentioned in Section 1. Compared with previous results, higher beam quality is normally realized in resonator structures employing FBGs. Using low-brightness LDs as a pump source is also beneficial toward achieving higher BE. The power output of resonators would be limited, however, by the available power of current LDs and the power endurance of FBGs. The amplifier structure has shown potential for power scaling, achieving up to a 2 kW power level. Furthermore, thanks to the degraded brightness of the pump fiber laser after power combination, a higher BE based on GRIN fiber RFA could be expected through further optimal design.

By utilizing GRIN fiber as the output fiber of the combiner, the mismatching of gain fiber and the combiner is eliminated, which is also employed in the resonator in Ref. [31]. Nevertheless, there is no specific design for seed injection, and thus it is not suitable for the MOPA system. Accordingly, in this demonstration, the original power combiner is replaced by a $(6 + 1) \times 1$ PSC. On one hand, the parameters of the tapered fused bundles are optimized with an adiabatic shape to satisfy the brightness conservation criterion and ensure high transmittance of the pump and seed lasers. On the other hand, the mode field matching between the input signal fiber and the GRIN fiber is carefully optimized. The central fiber of the input fibers used for seed injection is accurately fixed at the center of the bundle during the fabrication process. The bundles are then spliced directly with the GRIN fiber rather than the unmatched step-index fiber. Consequently, low insertion loss and superior beam quality preservation of the seed laser are realized by the aid of the optimized PSC. Finally, the ultimate beam quality of the RFA is effectively improved when compared with previous results. We achieve the best beam quality for GRIN RFLs of over 150 W. Meanwhile, it is the highest BE value among all high-power BE-enabled Raman lasers with over 100 W power.

5. Conclusions

Through utilizing the specially-designed PSC to optimize the injection of a seed laser, we achieve a BE-enabled RFA based on GRIN passive fiber with the best beam quality at 2 kW power level. The GRIN fiber-pigtailed PSC well preserves the seeding beam quality, and significantly helps enhance the brightness of the amplified laser. The maximum power output of the 1130 nm signal laser reaches 2.034 kW, with a high conversion efficiency of 79.35%. This is the highest conversion efficiency obtained for any GRIN Raman laser systems. The beam quality parameter M^2 remains ~2.8 at the maximum power output, and the corresponding BE reaches as high as ~11.2. We achieve the best beam quality for GRIN RFLs of over 150 W. It is also the highest BE value among high-power RFLs with over 100 W power.

Acknowledgements

This work was supported by Huo Yingdong Education Foundation (No. 151062), Hunan Provincial Innovation Construct Project (No. 2019RS3017), and National Natural Science Foundation of China (Nos. 11704409 and 61605246).

References

1. C. Jauregui, J. Limpert, and A. Tünnermann, Nat. Photonics **7**, 861 (2013).
2. M. N. Zervas and C. A. Codemard, IEEE J. Sel. Top. Quant. **20**, 219 (2014).
3. E. Stiles, in *Proceedings of the 5th International Workshop on Fiber Lasers* (2009), p. 4.
4. X. Chen, F. Lou, Y. He, M. Wang, Z. Xu, X. Guo, R. Ye, L. Zhang, C. Yu, L. Hu, B. He, and J. Zhou, Acta Optica Sinica **39**, 0336001 (2019).
5. Z. Liu, X. Jin, R. Su, P. Ma, and P. Zhou, Sci. China Inform. Sci. **62**, 41301 (2019).

https://doi.org/10.1017/hpl.2020.33 Published online by Cambridge University Press

6. G. P. Agrawal, *Nonlinear Fiber Optics*, 4th ed. (Academic Press, USA, 2006).
7. Y. Feng, *Raman Fiber Lasers* (Springer, Berlin, 2017).
8. V. R. Supradeepa, Y. Feng, and J. W. Nicholson, J. Opt. **19**, 23001 (2017).
9. Z. Wang, Q. Xiao, Y. Huang, J. Tian, D. Li, P. Yan, and M. Gong, High Power Laser Sci. Eng. **7**, e5 (2019).
10. V. R. Supradeepa and J. W. Nicholson, Opt. Lett. **38**, 2538 (2013).
11. J. Liu, F. Tan, H. Shi, and P. Wang, Opt. Express **22**, 28383 (2014).
12. J. Liu, D. Shen, H. Huang, C. Zhao, X. Zhang, and D. Fan, Opt. Express **22**, 6605 (2014).
13. W. Yao, B. Chen, J. Zhang, Y. Zhao, H. Chen, and D. Shen, Opt. Express **23**, 11007 (2015).
14. J. Dong, L. Zhang, H. Jiang, X. Yang, W. Pan, S. Cui, X. Gu, and Y. Feng, Opt. Express **26**, 5275 (2018).
15. J. Song, H. Wu, J. Ye, H. Zhang, J. Xu, P. Zhou, and Z. Liu, High Power Laser Sci. Eng. **6**, e28 (2018).
16. P. Ma, Y. Miao, W. Liu, D. Meng, and P. Zhou, Opt. Lett. **45**, 1974 (2020).
17. T. Yin, Z. Qi, F. Chen, Y. Song, and S. He, Opt. Express **28**, 7175 (2020).
18. E. A. Zlobina, S. I. Kablukov, A. A. Wolf, A. V. Dostovalov, and S. A. Babin, Opt. Lett. **42**, 9 (2017).
19. S. A. Babin, High Power Laser Sci. Eng. **7**, e15 (2019).
20. Y. Chen, T. Yao, L. Huang, H. Xiao, J. Leng, and P. Zhou, Opt. Express **28**, 3495 (2020).
21. C. A. Codemard, J. K. Sahu, and J. Nilsson, Proc. SPIE **7580**, 75801N (2010).
22. J. Liu, W. Yao, C. Zhao, D. Shen, and D. Fan, Appl. Opt. **53**, 8256 (2014).
23. Y. Glick, Y. Shamir, M. Aviel, Y. Sintov, S. Goldring, N. Shafir, and S. Pearl, Opt. Lett. **43**, 4755 (2018).
24. J. Ji, C. A. Codemard, M. Ibsen, J. K. Sahu, and J. Nilsson, IEEE J. Sel. Top. Quant. **15**, 129 (2009).
25. A. Polley and S. E. Ralph, IEEE Photonic. Tech. Lett. **19**, 218 (2007).
26. N. B. Terry, T. G. Alley, and T. H. Russell, Opt. Express **15**, 17509 (2007).
27. T. Yao, A. V. Harish, J. K. Sahu, and J. Nilsson, Appl. Sci. **5**, 1323 (2015).
28. Y. Glick, V. Fromzel, J. Zhang, A. Dahan, N. Ter-Gabrielyan, R. K. Pattnaik, and M. Dubinskii, Laser Phys. Lett. **13**, 065101 (2016).
29. Y. Glick, V. Fromzel, J. Zhang, N. Ter-Gabrielyan, and M. Dubinskii, Appl. Opt. **56**, B97 (2017).
30. E. A. Zlobina, S. I. Kablukov, A. A. Wolf, I. N. Nemov, A. V. Dostovalov, V. A. Tyrtyshnyy, D. V. Myasnikov, and S. A. Babin, Opt. Express **25**, 12581 (2017).
31. E. A. Evmenova, S. I. Kablukov, I. N. Nemov, A. A. Wolf, A. V. Dostovalov, V. A. Tyrtyshnyy, D. V. Myasnikov, and S. A. Babin, Laser Phys. Lett. **15**, 095101 (2018).
32. Y. Glick, Y. Shamir, A. A. Wolf, A. V. Dostovalov, S. A. Babin, and S. Pearl, Opt. Lett. **43**, 1027 (2018).
33. Y. Chen, J. Leng, H. Xiao, T. Yao, and P. Zhou, Laser Phys. Lett. **15**, 085104 (2018).
34. Y. Chen, J. Leng, H. Xiao, T. Yao, and P. Zhou, IEEE Access **7**, 28334 (2019).
35. Y. Chen, T. Yao, H. Xiao, J. Leng, and P. Zhou, Opt. Lett. **45**, 2367 (2020).
36. D. Neugroschl, J. Park, M. Wlodawski, J. Singer, and V. Kopp, Proc. SPIE **8601**, 860139 (2013).
37. K. Zhao, Z. Chen, X. Zhou, Z. Wang, and H. Jiang, Proc. SPIE **9532**, 953211 (2015).
38. S. Zou, H. Chen, H. Yu, J. Sun, P. Zhao, and X. Lin, Appl. Phys. B **123**, 288 (2017).
39. S. A. Babin, D. V. Churkin, A. E. Ismagulov, S. I. Kablukov, and E. V. Podivilov, Opt. Lett. **33**, 633 (2008).
40. Y. Glick, Y. Shamir, Y. Sintov, S. Goldring, and S. Pearl, Opt. Fiber Technol. **52**, 101955 (2019).

https://doi.org/10.1017/hpl.2020.33 Published online by Cambridge University Press